Saudi Journal of Civil Engineering
A Publication by “Scholars Middle East Publishers”, Dubai, United Arab Emirates
ISSN 2523-2657 (Print)
ISSN 2523-2231 (Online)

Improvement of Torsional Resistance in UHPC Beams by Tension Stiffening Index

Karim FR[1*], Abu Bakar, BH[2], Kok Keong, Choong[3], Aziz, OQ[4]
[1]Lecturer, Civil Engineering Department, College of Engineering, University of Sulaimani, Sulaimani, Iraq
[2]Professor, School of Civil Engineering, Universiti Sains Malaysia, Pulau Pinang, Malaysia
[3]Associated Professor, School of Civil Engineering, Universiti Sains Malaysia, Pulau Pinang, Malaysia
[4]Professor, Civil Engineering Department, College of Engineering, Salahaddin University, Erbil, Iraq

***Corresponding author**
Karim FR

Article History
Received: 04.09.2018
Accepted: 15.09.2018
Published: 30.10.2018

Abstract: The tension stiffening index is a critical factor which improved their effect on the torsional behavior of fibrous reinforced concrete beams which included the bond strength between the reinforcement and the concrete, and the amount of reinforcement indexes. Thus, this paper highlights the effect of the tension stiffening index on the torsional resistance of ultra-high performance fiber reinforced concrete (UHPFRC) beams under pure torsion. Therefore, four under-reinforced ultra-high performance fiber reinforced concrete beams were cast and tested under pure torsion which contains the fixed amount of longitudinal and transverse reinforcements, while the grade and the rib pattern on the surface of reinforcement have been changed. Test results verified that the torsional resistance, stiffness of the cracked section and the twisting angle were improved at the crack and peak loads due to a reduction in the tension stiffening index. However, the axial strains in transverse and longitudinal reinforcements.

Keywords: Pure torsion, Reinforcement index, Tension stiffening index, and Ultra-high performance fiber reinforced concrete.

List of notation

f_{bt}: Bond strength between transverse reinforcement and the matrix of ultra-high performance fiber reinforced concrete, MPa
f_{bL}: Bond strength between the longitudinal reinforcement and the matrix of ultra-high performance fiber reinforced concrete, MPa
$LVDT$: Linear variable differential transformer
TSI: Tension stiffening index, MPa
VC: Visco Crete
UH: Ultra-High Performance fiber reinforced concrete
$\rho_t f_{ty}$: Transverse reinforcement index, MPa
$\rho_L f_{Ly}$: Longitudinal reinforcement index, MPa
Φ: diameter of fiber, mm

INTRODUCTION

Non-fibrous concrete beams are designed for resisting torsional moment, the compressive strength and dimensions of the section are taken into account before cracking, while the yield stress of transverse reinforcement in stress-strain curve, stirrup dimensions and spacing between stirrups are considered at peak load [1, 2]. In contrast, the compressive strength and split tensile strength in fibrous concrete were influenced by the inclusion of steel fiber [3-5]. Consequently, the bond strength between reinforcement and the matrix of fibrous concrete improved proportionally with compressive strength [6]. However, the spacing between spiral cracks and the width of crack at failure were influenced by the bond strength between reinforcement and the matrix of concrete [7]. Although, the amount of reinforcement has effect on the strain in reinforcement [2], the strain in reinforcement embedded steel bar in concrete was less than the strain of reinforcement corresponding to yield stress in stress-strain curve which is known as tension stiffening [8]. In addition, the strain in longitudinal reinforcement has been influenced on the shear strain in diagonal compression strut

[9]. Thus, the value of bond strength and the amount of reinforcement indexes have influence on the tension stiffening index and torsional resistance as a result. The tension stiffening index is expressed as follows:

$$TSI = \frac{f_{bt}(\rho_t f_{ty} + \rho_L f_{Ly})}{f_{bL}} \qquad (1)$$

Research Significance

The inclusion of micro steel fiber has been found to improve the bond strength between reinforcement bars and the matrix of ultra-high performance concrete and reduce the strain in steel reinforcement due to tension stiffening even though the embedded reinforcements have been high yield stress. The torsional behavior of under-reinforced concrete beams is influenced by the inclusion of steel fiber in ultra-high performance concrete. Thus, this paper highlights the influence of tension stiffening index on the torsional behavior of under-reinforced ultra-high performance fiber reinforced concrete beams.

Experimental works

To be certain about the influence of tension stiffening index on the torsional resistance in under-reinforced ultra-high performance fiber reinforced concrete beams, four beams were cast and tested under pure torsional moment. The beam was denoted as B-1*-UH, D-1-UH, D-2-UH and D-3-UH where all of them contain the same amount of reinforcements and fiber. The only difference was in the steel reinforcement bars where the value of the yield stress in stress-strain curve is different. The mix proportion of materials, detail of beam layout and reinforcements, procedure of fabrication of specimens and testing of beams under pure torsion are described in the following sections:

Mix proportion of materials in ultra-high performance fiber reinforced concrete

The design compressive strength of ultra-high performance fiber reinforced concrete beams was 127 MPa. The materials used for producing this concrete, including type I Ordinary Portland Cement, silica sand (0.6 mm maximum sieve size), silica flour (11.9μm median particle size), silica fume, HRWR Sika Vicocrete 2055, Retard-admixture Plastiment R, tap water and two sizes of copper coated micro steel fiber A and B. The proportioning of these materials and the details of micro steel fiber are shown in Table-1.

Table-1: Mix proportion of ultra-high performance fiber reinforced concrete

Materials	**Quantity , kg/m^3**
Cement (Type I)	1500
Quartz sand 0.6 mm	539.5
Quartz sand 0.325 mm	110.5
Silica fume	175
Silica flour	126.08
Water	372.76
Water reduces super-plasticizer VC2055	38.23
Retard-admixture (Plastiment-R)	7.49
Micro steel fiber, A(21mmX 0.35mmΦ)	26.50
Micro steel fiber, B (12mm X 0.20mmΦ)	150.13
Slump-flow, mm [10]	720

Details of reinforcements and the beam layout

The engineering properties of steel reinforcements which were used for fabricating the four beams are shown in Table-2. Four bars of 12 mm diameter were used as longitudinal reinforcement in the main beams which were closed by transverse reinforcement 6 mm diameter bars with 216 mm height and 166 mm width ended with 135º standard hooks. Meanwhile, the spacing between transverse reinforcement was 95 mm as shown in Figure 1. The dimensions of the four beams are tabulated in Table-3. In addition, the clear span to depth ratio and height to width ratio of the beam section are kept constant at 5.7 and 1.2, respectively.

Table-2: Engineering properties of steel reinforcements

Code	Approximate diameter, (mm)	Measured diameter, (mm)	Pitch per 10	Thickness of the rib, (mm)	Mass per length, (kg/m)	% of elongation	Yield strength, (MPa)	Ultimate strength, (MPa)	Modulus of elasticity, (MPa)
$A1_p$	6	6.20	0.0	0.000	0.247	6.37	602.78	628.32	201411
A2	6	6.17	2.2	0.320	0.234	11.10	417	514.88	207010
B1	12	11.45	1.5	0.590	0.853	12.34	586.64	675.01	192218
B2	12	11.17	1.2	0.595	0.712	16.97	422.03	505.84	196444

$_p$: Plain reinforcement

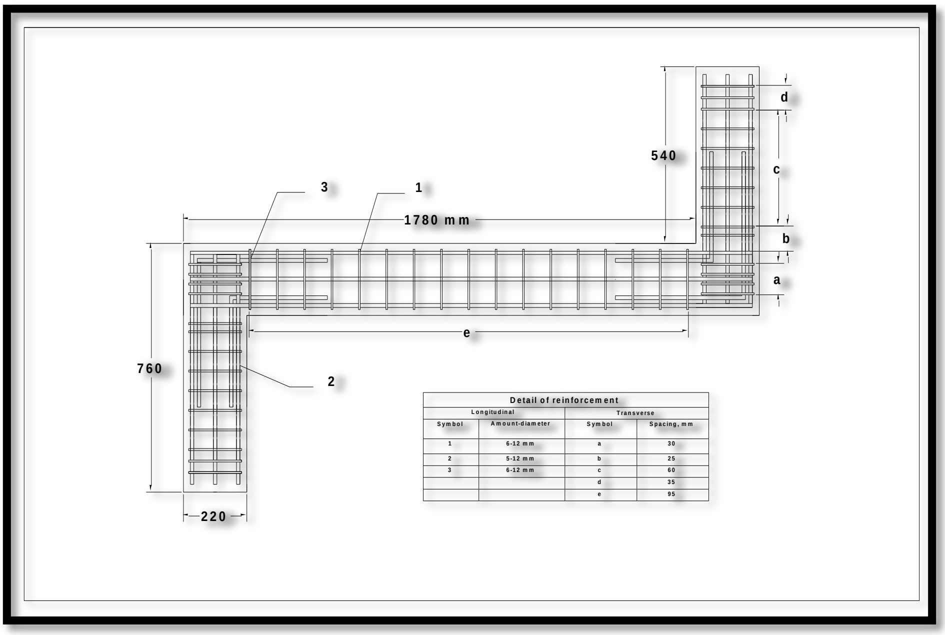

Fig-1: Detail of reinforcements in the fibrous concrete beam

Fabrication of specimens and curing regimes

The materials were used to produce ultra-high performance fiber reinforced concrete. They were mixed in the sequence and elapse time as shown in Figure-2. The beams were cast by two pan mixers 0.05 m^3. The ultra-high performance fiber reinforced concrete beam was cast and it was associated with three cubes for compression test, three cylinders for split tensile test, three prisms for flexural test and six cubes for pullout test. The ultra-high performance fiber reinforced concrete beams were cast in four layers inside of a plywood mold. Each layer was externally vibrated for 45 seconds at different points along the length of the beam. The cast ultra-high performance fiber reinforced concrete beams were removed from the mold after 12 hours of casting. Then, the beams were kept in steam curing chamber for 36 hours at 55ºC. Next, the concrete beams were removed from steam curing chamber and were covered by wetted burlap for 132 hours.

Table-3: Measured dimensions of the fibrous concrete beams

Beam denotation	Concrete cover, mm	Width, mm	Height, mm	Span length, mm
B-1*-UH	21	214	264	1533
D-1-UH	26	224	274	1568
D-2-UH	25	222	272	1564
D-3-UH	25	222	272	1564

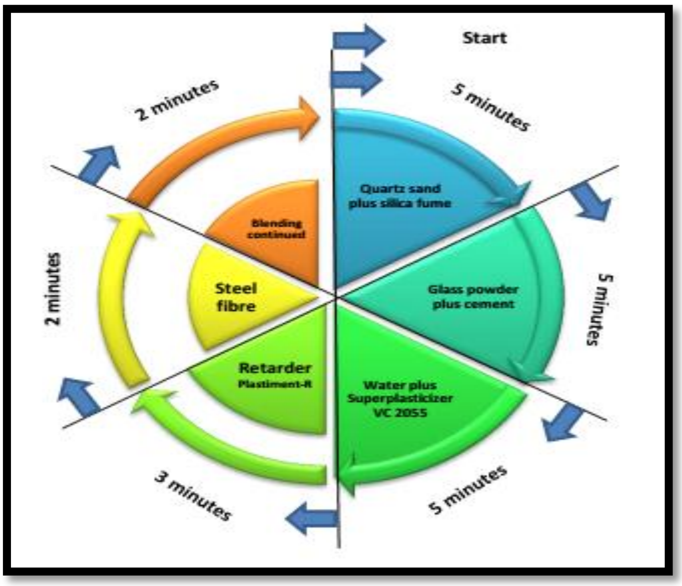

Fig-2: Sequence of mixing materials in ultra-high performance fiber reinforced concrete

Testing of beam under-pure torsional moment

To produce pure torsional moment on the main beams, the loading set-up was arranged as shown in Figure 3 & 4. The twisting angle was measured from displacement recorded using LVDTs on a steel frame which was clamped on the section of the beam as shown in Figure-5.

The strains in reinforcements were measured by electrical strain gauges during the loading. The Universal Testing Machine of 500 kN capacity was used for testing of beams. The under-reinforced ultra-high performance fiber reinforced concrete beams were set on the two saddle supports. The load was applied to the load spreader beam first. Then, the load was transferred to the reinforced concrete arms which produced a pure torsional moment on the main beam as a result. The load was increased manually until the beam failed under torsional moment.

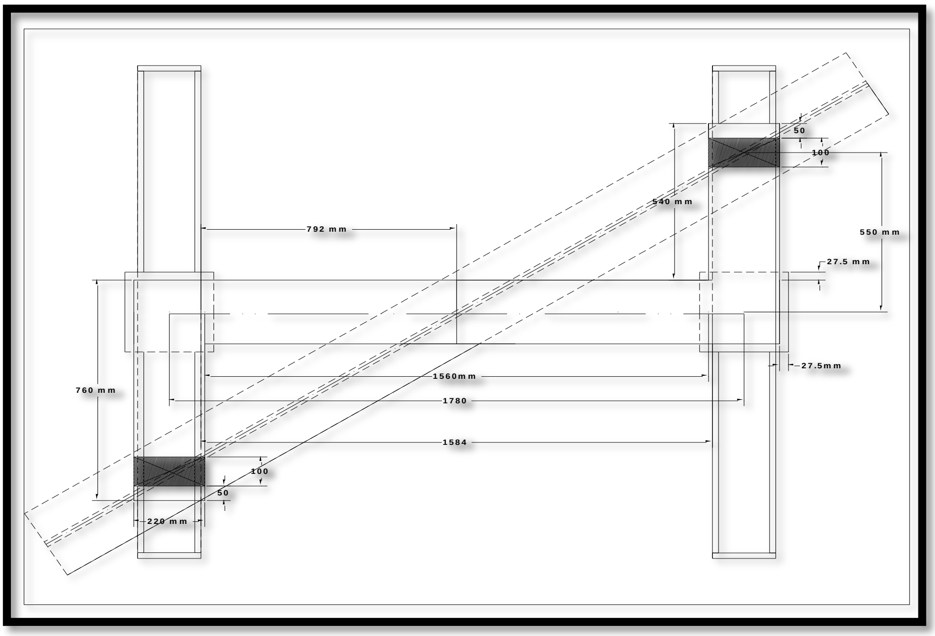

Fig-3: Schematic Test set-up

Fig-4: Loading set-up of the beams

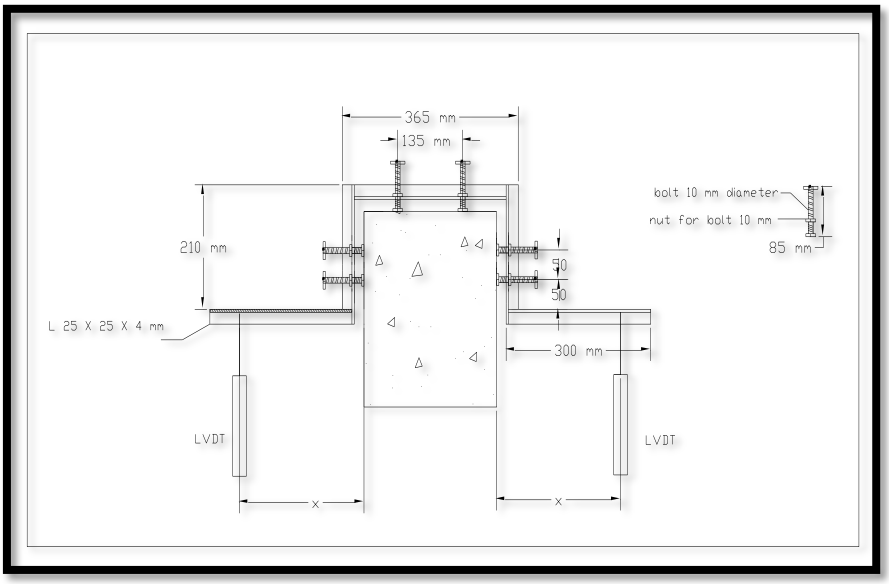

Fig-5: Schematic measure of twisting angle of the beam section

RESULTS AND DISCUSSIONS

The mechanical properties of ultra-high performance fiber reinforced concrete were determined for each tested beams. In addition, the properties of steel bars with bond strength between steel reinforcements and the matrix of ultra-high performance fiber reinforced concrete were measured as shown in Table 4 and 5 [11-15]. The value of torsional resistance and twisting angle were measured at crack and peak loads. The stiffness of the section at crack load for each beam which was calculated based on elastic theory are tabulated in Table-6 [16].

The influence of bond strength between reinforcements and matrix of ultra-high performance fiber reinforced concrete and the amount of reinforcement indexes on the torsional behavior of ultra-high performance fiber reinforced concrete beams is known as tension stiffening index (*TSI*). The influence of tension stiffening index on torsional resistance, twisting angle, shear strain in concrete, strain in reinforcements and details of spiral cracks pattern is described in the following sections:

Table-4: Measured mechanical properties of ultra-high performance fiber reinforced concrete with respect to tested beams

Beam denotation	$f_{c'cube}$, MPa	f_{sp}, MPa	f_r, MPa
B-1-UH	127.5	10.33	12.84
D-1-UH	127.7	17.05	16.82
D-2-UH	132.3	18.22	10.34
D-3-UH	131.3	15.05	9.85

Table-5: Tension stiffening index for ultra-high performance fiber reinforced concrete beams

Beam denotation	Transverse reinforcement		Longitudinal reinforcement		TSI*, MPa
	$\rho_t f_{ty}$, MPa	f_{bt}, MPa	$\rho_L f_{Ly}$, MPa	f_{bL}, MPa	
B-1-UH	1.771	7.362	4.386	11.573	3.731
D-1-UH	2.379	9.486	4.036	15.818	3.982
D-2-UH	2.418	5.720	5.994	19.514	2.511
D-3-UH	1.657	7.127	5.995	19.147	2.900

Table-6: Results of pure torsion test of under-reinforced ultra-high performance fiber reinforced concrete beams

Beam denotation	T_{cr}, kN.m	Φ_{cr}, rad/m, X 10^{-3}	T_u, kN.m	Φ_u, rad/m, X 10^{-3}	K_{cr}, kN.m/rad.
B-1-UH	12.11	5.655	24.96	37.280	406.3
D-1-UH	17.50	6.353	24.46	51.285	154.9
D-2-UH	13.40	3.324	28.97	40.825	415.1
D-3-UH	9.97	0.153	26.97	34.837	490.3

Torsional resistances at the crack and peak loads

It can be seen in Figure 6 that the cracking torsional resistance of ultra-high performance fiber reinforced concrete beams was not only influenced by the compressive strength of concrete. The tension stiffening index was found to have influenced on the torsional resistance at crack load as well.

It was found that the cracking torsional resistance was improved up to 30.5% due to increases in the tension stiffening index from 2.511 to 3.731 MPa. Meanwhile, the compressive strength of ultra-high performance fiber reinforced concrete decreased in the range of 3.6%. In contrast, the ultimate torsional resistance was influenced by tension stiffening index as well as shown in Figure 7. It is observed that the torsional resistance was improved up to 18.42% due to a reduction in tension stiffening index from 3.982 MPa to 2.511 MPa.

Twisting angles at crack and peak loads

Basically, the twisting angle varied with torsional loading as shown in Figure 8. Twisting angle at crack load was reduced up to 47.6% due to improvement of stiffness by up to 31.6% and a reduction in tension stiffening index from 3.982 MPa to 2.511MPa. In contrast, the twisting angle at peak load was reduced up to 20.4% due to improvement in stiffness of the cracked section of up to 167% and a reduction in tension stiffening index from 3.982 MPa to 2.511 MPa.

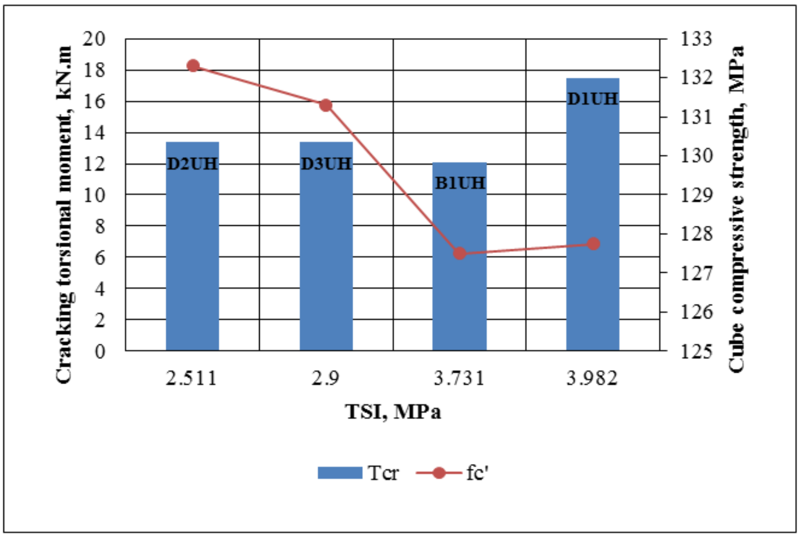

Fig-6: Effect of tension stiffening index and compressive strength of the cracking torsional resistance

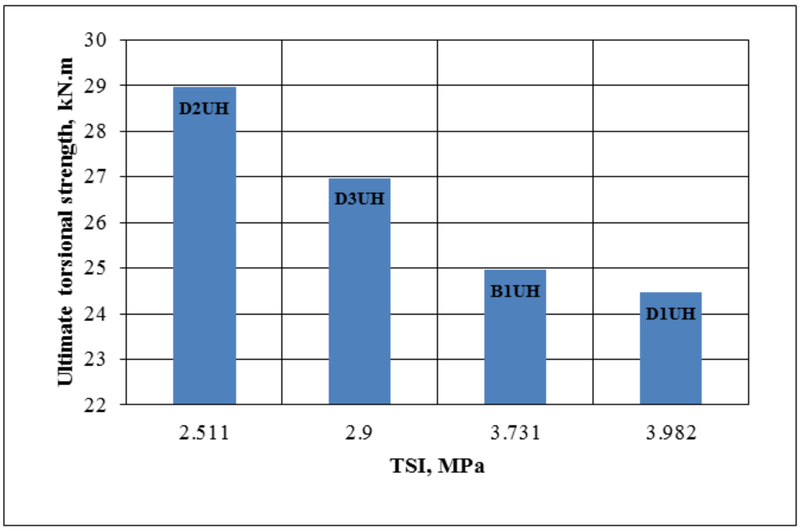

Fig-7: Influence of tension stiffening index on the torsional resistance at peak load

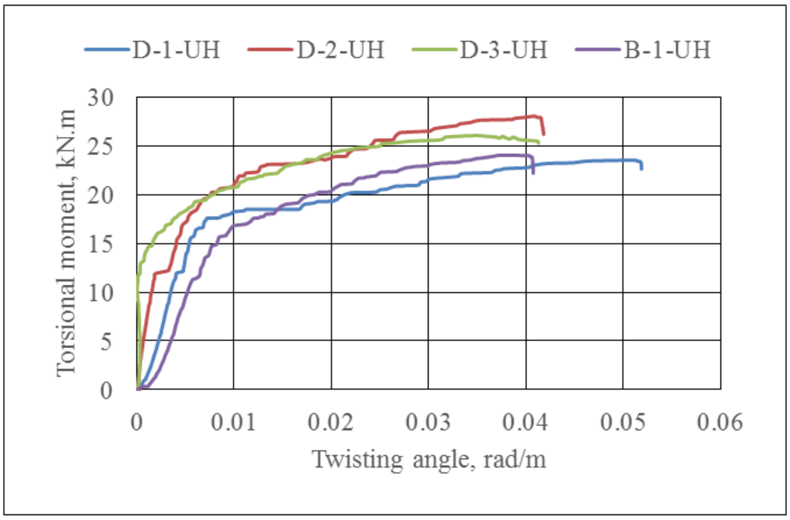

Fig-8: Torsional moment versus twisting angle

Strain in fibrous concrete

The value of the tension stiffening index influenced the shear strain in ultra-high performance fiber reinforced concrete, even though the cube compressive strength of ultra-high performance fiber reinforced concrete was still in the same range as shown in Figure 9. The strain in concrete at the crack and peak loads and the compressive strain in diagonal concrete strut are shown in Table-7. It was observed that the ultra-high performance fiber reinforced concrete was crushed under torsional loading because the compressive strain in the diagonal compression concrete strut exceeded the ultimate strain of ultra-high performance fiber reinforced concrete.

Table-7: Strain in fibrous concrete

Beam denotation	Shear strain, mm/mm X 10^{-6}		Strain in diagonal compression strut, mm/mm X 10^{-6}
	At crack load	At peak load	
B-1-UH	1170	37120	-0.014329
D-1-UH	3021	223020	-0.118068
D-2-UH	3372	27148	-0.013509
D-3-UH	2333	20165	-0.008871

-ve: compression

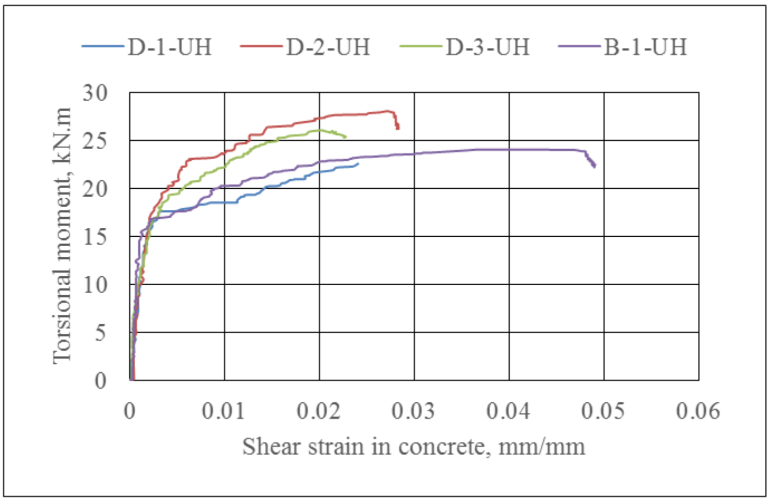

Fig-9: Torsional moment versus shear strain in concrete

Strains in longitudinal and transverse reinforcements

The strains in transverse and longitudinal reinforcements were influenced by the tension stiffening index as shown in Figure 10 and 11. It was observed that the strains in transverse and longitudinal reinforcement were reduced up to 59.29% and 74.53%, respectively. The reduction in reinforcement strain was due to a reduction in tension stiffening index from 3.982 MPa to 2.511 MPa.

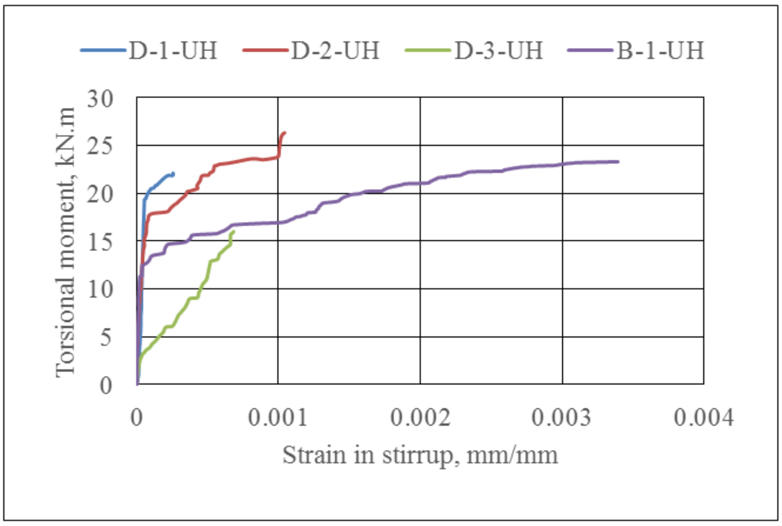

Fig-10: Torsional moment versus strain in transverse reinforcement

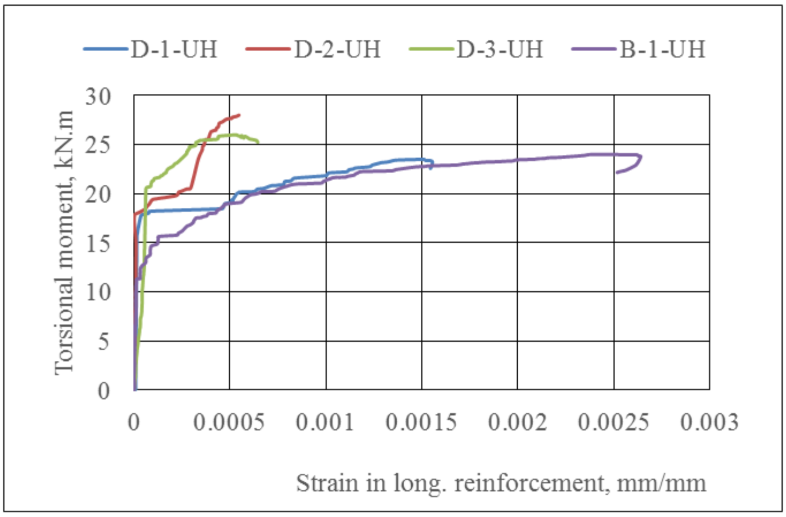

Fig-11: Torsional moment versus strain in the longitudinal reinforcement

Cracking patterns

The details of spiral cracks were affected by tension stiffening index as shown in Table 8. It was observed that the average spacing between spiral cracks, number of spiral cracks, and angle of inclination of crack at failure changed with the amount of the transverse reinforcement index. In addition, it was found that the angle of inclination of crack and the average spacing increased due to improvement of transverse reinforcement index, and the number of spiral cracks was reduced as a result.

The final features of crack at the failure of ultra-high performance fiber reinforced concrete beams under pure torsional loading influenced by tension stiffening indexes are shown in Figure 12-15.

Table-8: Details of spiral cracks of ultra-high performance fiber reinforced concrete beams

Beam denotation	No. of spiral cracks	Angle of inclination of crack at failure, degrees	Average spacing between spiral cracks, mm
B-1-UH	14	42	95
D-1-UH	6	47	231
D-2-UH	11	46	122
D-3-UH	13	43	109

Fig-12: Crack pattern of beam B-1*-UH at failure

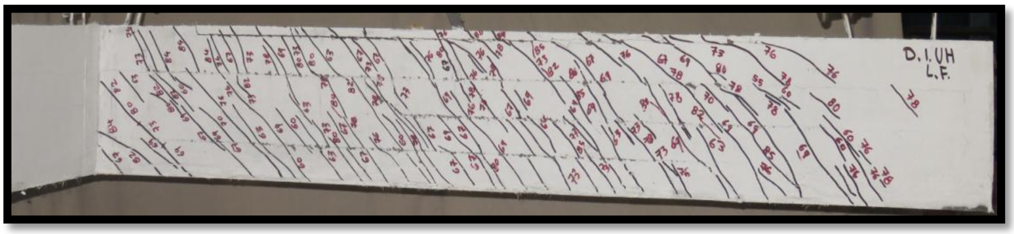

Fig-13: Crack pattern of beam D-1-UH at failure

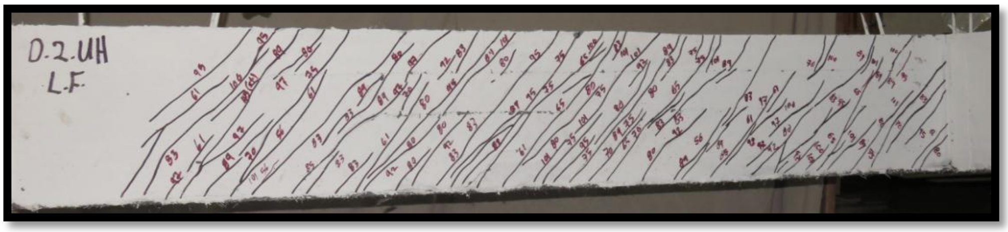

Fig-14: Crack pattern of beam D-2-UH at failure

Fig-15: Crack pattern of beam D-3-UH at failure

CONCLUSIONS

Based on the test results of under-reinforced ultra-high performance fiber reinforced concrete beams under pure torsional moment, the following conclusions on the torsional behavior could be drawn:

- The cracking torsional resistance was improved up to 30.5% due to increases in the tension stiffening index. In contrast, torsional resistance at peak load was enhanced up to 18.42% due to a reduction in the tension stiffening index.
- The twisting angle of under-reinforced ultra-high performance fiber reinforced concrete beams at the crack and ultimate loads decreased due to improvement in section stiffness and reduction of tension stiffening index at the same time.
- It was found that the under-reinforced concrete beams crushed before yielding in reinforcement at the end of torsion test due to high value of the brittleness index in ultra-high performance fiber reinforced concrete.
- The value of transverse reinforcement index improved the spacing between spiral cracks and inclination angle of the crack at failure. Consequently, the number of spiral cracks was reduced as a result.

ACKNOWLEDGMENT

This work was conducted as part of the doctoral studies of the first author. The PhD program has been financially supported by Kurdistan Government Region-Iraq and School of Civil Engineering, Universiti Sains Malaysia which are gratefully acknowledged.

REFERENCES

1. ACI Committee. Building code requirements for structural concrete (ACI 318M-14): an ACI Standard: Commentary on building code requirements for structural concrete (ACI 318M-14). 2015. *Farmington Hills, MI: American Concrete Institute*.
2. Hsu, T. T., & Mo, Y. L. (1985). Softening of concrete in torsional members-design recommendations. In *Journal Proceedings* (Vol. 82, No. 4, pp. 443-452).
3. Karim, F. K., Abu Bakar, B. H., & Kok Keong, C. (2016). Influence of fiber size on the compressive and split tensile strengths of fibrous normal strength concrete. *1st International conference on Engineering and Innovative Technology*. Erbil, Kurdistan-Iraq.
4. Karim, F. K., Abu Bakar, B. H., & Kok Keong, C. (2016). Influence of size and volume fraction of fiber on the compressive and split tensile strength of SFHSC. *ARPN Journal of Science and Technology,* 6**,** 114-122.
5. Karim, F. K., Abu Bakar, B. H., Kok Keong, C., & Aziz, O. Q. (2016). Influence of fiber size on the compressive strength of ultra-high performance concrete. *International Journal of Emerging Technology and Advanced Engineering,* 6**,** 199-203.
6. Harajli, M. H., & Mabsout, M. E. (2002). Evaluation of Bond Strength of Steel Reinforcing Bars in Plain and Fiber-Reinforced Concrete. *ACI Structural Journal,* 99**,** 509-517.
7. Park, S. K., Ko, W. J., & Kim, H. Y. (2001). Estimation of torsional crack width for concrete structural members. *Magazine of Concrete Research*, *53*(5), 337-345.
8. Maekawa, K., Pimanmas, A., & Okamura, H. (2002). *Nonlinear mechanics for concrete structures,* London, E & FN Spon.
9. Rao, T. D., & Rama Seshu, D. (2005). Analytical model for the torsional response of steel fiber reinforced concrete members under pure torsion. *Cement & Concrete Composites,* 27**,** 493-501.
10. ASTM, C. (2009). Standard test method for slump flow of self-consolidating concrete.
11. ASTM, S. (2009). *Standard specification for deformed and plain carbon-steel bars for concrete reinforcement*.
12. ASTM-C496/C496M. (2004). Standard Test Method for Splitting Tensile Strength of Cylindrical Concrete Specimens. *Annual book of ASTM standard, C496/C496M,* 4.02**,** 299-303.
13. ASTM, I. (2010). Standard test method for flexural performance of fiber-reinforced concrete (using beam with third-point loading). *United States*.
14. BSI:12390. (2002). Compressive strength of test specimens. *British Standard Testing Concrete,* BS EN 12390**,** 1-14.
15. IS:2770. (2007). Methods of Testing Bond in reinforced concrete: Pullout test. *Bureau of Indian Standards,* 2770**,** 1-10.
16. Fang, I. K., & Shiau, J. K. (2004). Torsional behavior of normal-and high-strength concrete beams. *Structural Journal*, *101*(3), 304-313.